

A DOUBLY RELAXED MINIMAL-NORM GAUSS-NEWTON METHOD FOR UNDERDETERMINED NONLINEAR LEAST-SQUARES PROBLEMS

FEDERICA PES* AND GIUSEPPE RODRIGUEZ*

Abstract. When a physical system is modeled by a nonlinear function, the unknown parameters can be estimated by fitting experimental observations by a least-squares approach. Newton's method and its variants are often used to solve problems of this type. In this paper, we are concerned with the computation of the minimal-norm solution of an underdetermined nonlinear least-squares problem. We present a Gauss-Newton type method, which relies on two relaxation parameters to ensure convergence, and which incorporates a procedure to dynamically estimate the two parameters, as well as the rank of the Jacobian matrix, along the iterations. Numerical results are presented.

Key words. nonlinear least-squares problem, minimal-norm solution, Gauss-Newton method, parameter estimation

AMS subject classifications. 65H10, 65F22

1. Introduction. Let us assume that $F(\mathbf{x}) = [F_1(\mathbf{x}), \dots, F_m(\mathbf{x})]^T$ is a nonlinear twice continuously Frechét-differentiable function with values in \mathbb{R}^m , for any $\mathbf{x} \in \mathbb{R}^n$. For a given $\mathbf{b} \in \mathbb{R}^m$, we consider the nonlinear least-squares data fitting problem

$$\min_{\mathbf{x} \in \mathbb{R}^n} \|\mathbf{r}(\mathbf{x})\|^2, \quad \mathbf{r}(\mathbf{x}) = F(\mathbf{x}) - \mathbf{b}, \quad (1.1)$$

where $\|\cdot\|$ denotes the Euclidean norm and $\mathbf{r}(\mathbf{x}) = [r_1(\mathbf{x}), \dots, r_m(\mathbf{x})]^T$ is the residual vector function between the model expectation $F(\mathbf{x})$ and the vector \mathbf{b} of measured data. The solution to the nonlinear least-squares problem gives the best model fit to the data in the sense of the minimum sum of squared errors. A common choice for solving a nonlinear least-squares problem consists of applying Newton's method and its variants, such as the Gauss-Newton method [2, 12, 13].

The Gauss-Newton method is based on the construction of a sequence of linear approximations to $\mathbf{r}(\mathbf{x})$. Chosen an initial point $\mathbf{x}^{(0)}$ and denoting by $\mathbf{x}^{(k)}$ the current approximation, then the new approximation is

$$\mathbf{x}^{(k+1)} = \mathbf{x}^{(k)} + \mathbf{s}^{(k)}, \quad k = 0, 1, 2, \dots, \quad (1.2)$$

where the step $\mathbf{s}^{(k)}$ is computed as a solution to the linear least-squares problem

$$\min_{\mathbf{s} \in \mathbb{R}^n} \|J(\mathbf{x}^{(k)})\mathbf{s} + \mathbf{r}(\mathbf{x}^{(k)})\|^2. \quad (1.3)$$

Here $J(\mathbf{x})$ represents the Jacobian matrix of the function $F(\mathbf{x})$.

The solution to (1.3) may not be unique: this happens when the matrix $J(\mathbf{x}^{(k)})$ does not have full column rank, in particular, when $m < n$. To make the solution unique, the new iterate $\mathbf{x}^{(k+1)}$ is often obtained by solving the following minimal-norm linear least-squares problem

$$\begin{cases} \min_{\mathbf{s} \in \mathbb{R}^n} \|\mathbf{s}\|^2 \\ \mathbf{s} \in \left\{ \arg \min_{\mathbf{s} \in \mathbb{R}^n} \|J(\mathbf{x}^{(k)})\mathbf{s} + \mathbf{r}(\mathbf{x}^{(k)})\|^2 \right\}, \end{cases} \quad (1.4)$$

*Department of Mathematics and Computer Science, via Ospedale 72, 09124 Cagliari, Italy,
 federica.pes@unica.it, rodriguez@unica.it

where the set in the lower line contains all the solutions to problem (1.3).

In order to select solutions exhibiting different degrees of regularity, the term $\|\mathbf{s}\|^2$ in (1.4) is sometimes substituted by the seminorm $\|L\mathbf{s}\|^2$, where $L \in \mathbb{R}^{p \times n}$ ($p \leq n$) is a matrix which incorporates available a priori information on the solution. The case $p > n$ can be easily reduced to the previous assumption by performing a compact $L = QR$ factorization, and substituting L by the triangular matrix R . Typically, L is a diagonal weighting matrix or a discrete approximation of a derivative operator. For example, the matrices

$$D_1 = \begin{bmatrix} 1 & -1 & & & \\ & \ddots & \ddots & & \\ & & 1 & -1 & \end{bmatrix} \quad \text{and} \quad D_2 = \begin{bmatrix} 1 & -2 & 1 & & \\ & \ddots & \ddots & \ddots & \\ & & 1 & -2 & 1 \end{bmatrix}, \quad (1.5)$$

of size $(n-1) \times n$ and $(n-2) \times n$, respectively, are approximations to the first and second derivative operators. When a regularization matrix is introduced, problem (1.4) becomes

$$\begin{cases} \min_{\mathbf{s} \in \mathbb{R}^n} \|L\mathbf{s}\|^2 \\ \mathbf{s} \in \left\{ \arg \min_{\mathbf{s} \in \mathbb{R}^n} \|J(\mathbf{x}^{(k)})\mathbf{s} + \mathbf{r}(\mathbf{x}^{(k)})\|^2 \right\}. \end{cases} \quad (1.6)$$

Both (1.4) and (1.6) impose some kind of regularity on the update vector \mathbf{s} for the solution $\mathbf{x}^{(k)}$ and not on the solution itself. The problem of imposing a regularity constraint directly on the solution \mathbf{x} of problem (1.1), i.e.,

$$\begin{cases} \min_{\mathbf{x} \in \mathbb{R}^n} \|\mathbf{x}\|^2 \\ \mathbf{x} \in \left\{ \arg \min_{\mathbf{x} \in \mathbb{R}^n} \|F(\mathbf{x}) - \mathbf{b}\|^2 \right\}, \end{cases} \quad (1.7)$$

is studied in [6, 7, 8, 14]. These papers are based on the application of the damped Gauss–Newton method to the solution of (1.7). To ensure the computation of the minimal-norm solution, at the k th iteration, the Gauss–Newton approximation is orthogonally projected onto the null space of the Jacobian $J(\mathbf{x}^{(k)})$. In [14], the damping parameter is estimated by the Armijo–Goldstein principle; we refer to this method as the MNGN algorithm. In the same paper, this approach is applied to the minimization of a suitable seminorm, and different regularization techniques are considered under the assumption that the nonlinear function F is ill-conditioned.

Unfortunately, the algorithms developed in the above papers, which take the form

$$\mathbf{x}^{(k+1)} = \mathbf{x}^{(k)} + \alpha_k \tilde{\mathbf{s}}^{(k)} - V_2 V_2^T \mathbf{x}^{(k)},$$

occasionally lack to converge. One reason is that the projection step may cause the residual to increase considerably at particular iterations. Moreover, the rank of $J(\mathbf{x}^{(k)})$ may vary as the iteration progresses, and its incorrect estimation often leads to the presence of small singular values for the Jacobian, which amplify computational errors.

This problem of nonconvergence is dealt with in [3], by a method which will be denoted CKB in the following. The authors consider a convex combination of the Gauss–Newton approximation and its orthogonal projection, and apply a relaxation parameter to this search direction, chosen according to a given rule. After some manipulation, the method can be written as

$$\mathbf{x}^{(k+1)} = \mathbf{x}^{(k)} + \tilde{\mathbf{s}}^{(k)} - \gamma_k V_2 V_2^T \mathbf{x}^{(k)}. \quad (1.8)$$

This approach makes the computation of the minimal-norm solution more robust, but it may not converge in some situation; see Section 4. Moreover, both the MNGN and the CKB methods suffer from serious convergence problems caused by the variation of the rank of the Jacobian along the iterations, which often drops to a small value in a neighborhood of the solution.

In this paper, we aim at improving the convergence of the methods presented in [3] and [14]. We do this by first introducing in the MNGN method a technique to estimate the rank of the matrix $J(\mathbf{x}^{(k)})$ at each iteration. This procedure has the effect of improving the convergence of the method, reducing the possibility that the iteration diverges because of error amplification. Then, we introduce a second relaxation parameter for the projection term, as well as a strategy to automatically tune it, besides the usual damping parameter for the Gauss–Newton search direction. This approach produces, on the average, solutions closer to optimality, i.e., with smaller norms, than those computed by the CKB method. Furthermore, we consider a model profile $\bar{\mathbf{x}}$ for the solution, which is useful in applications where sufficient a priori information on the physical system under investigation is available.

The paper is structured as follows. In Section 2, we revise the MNGN method and reformulate Theorem 3.1 from [14] by introducing a model profile for the solution. Then, we give a theoretical justification for the fact that the convergence of the method may not be ensured. Section 3 explains how to estimate the numerical rank of the Jacobian $J(\mathbf{x}^{(k)})$ at each iteration. In Section 4, we describe an algorithm which introduces a second parameter to control the size of the correction vector that provides the minimal-norm solution, and which estimates automatically such parameter. In Section 5, we extend the discussion to the minimal- L -norm solution, where L is a regularization matrix. Numerical examples can be found in Section 6.

2. Nonlinear minimal-norm solution. We begin by recalling the definition of the singular value decomposition (SVD) of a matrix $J \in \mathbb{R}^{m \times n}$ [10], which will be needed later. The SVD is a matrix decomposition of the form

$$J = U\Sigma V^T,$$

where $U = [\mathbf{u}_1, \dots, \mathbf{u}_m] \in \mathbb{R}^{m \times m}$ and $V = [\mathbf{v}_1, \dots, \mathbf{v}_n] \in \mathbb{R}^{n \times n}$ are matrices with orthonormal columns and $\Sigma_{i,j} = 0$ for $i \neq j$. The nonzero diagonal elements of the matrix $\Sigma \in \mathbb{R}^{m \times n}$ are the *singular values* $\sigma_1 \geq \sigma_2 \geq \dots \geq \sigma_r > 0$, with $r = \text{rank}(J) \leq \min(m, n)$. Let $\mathcal{N}(J)$ denote the null space of the matrix J . It is well-known that

$$\mathcal{N}(J) := \{\mathbf{s} \in \mathbb{R}^n : J\mathbf{s} = 0\} = \text{span}\{\mathbf{v}_{r+1}, \dots, \mathbf{v}_n\}.$$

Let us now briefly review the computation of the minimal-norm solution to the nonlinear problem (1.1) by the *minimal-norm Gauss–Newton* (MNGN) method, presented in [14]. Our aim is showing the reason for the possible lack of convergence of such method. Here, we extend the discussion from [14] by introducing a model profile $\bar{\mathbf{x}} \in \mathbb{R}^n$, which represents an a priori estimate of the desired solution, and formulate the problem in the form

$$\begin{cases} \min_{\mathbf{x} \in \mathbb{R}^n} \|\mathbf{x} - \bar{\mathbf{x}}\|^2 \\ \mathbf{x} \in \{\arg \min_{\mathbf{x} \in \mathbb{R}^n} \|F(\mathbf{x}) - \mathbf{b}\|^2\}. \end{cases} \quad (2.1)$$

We consider an iterative method of the type (1.2) based on the following first-order

linearization of the problem

$$\begin{cases} \min_{\mathbf{s} \in \mathbb{R}^n} \|\mathbf{x}^{(k)} - \bar{\mathbf{x}} + \alpha_k \mathbf{s}\|^2 \\ \mathbf{s} \in \{\arg \min_{\mathbf{s} \in \mathbb{R}^n} \|J_k \mathbf{s} + \mathbf{r}_k\|^2\}, \end{cases} \quad (2.2)$$

where $J_k = J(\mathbf{x}^{(k)})$ is the Jacobian of F in $\mathbf{x}^{(k)}$ and $\mathbf{r}_k = \mathbf{r}(\mathbf{x}^{(k)})$ is the residual vector.

The damping parameter α_k is indispensable to ensure the convergence of the Gauss–Newton method. We estimate it by the Armijo–Goldstein principle [1, 9], but it can be chosen by any strategy which guarantees a reduction in the norm of the residual. In our case, the Armijo condition [1, 5] implies

$$f(\mathbf{x}^{(k)} + \alpha_k \tilde{\mathbf{s}}^{(k)}) \leq f(\mathbf{x}^{(k)}) + \mu \alpha_k \nabla f(\mathbf{x}^{(k)})^T \tilde{\mathbf{s}}^{(k)},$$

where $\tilde{\mathbf{s}}^{(k)}$ is determined by solving (1.4) and μ is a constant in $(0, 1)$. Since $f(\mathbf{x}) = \frac{1}{2} \|\mathbf{r}(\mathbf{x})\|^2$ and $\nabla f(\mathbf{x}) = J(\mathbf{x})^T \mathbf{r}(\mathbf{x})$, it reads

$$\|\mathbf{r}(\mathbf{x}^{(k)} + \alpha_k \tilde{\mathbf{s}}^{(k)})\|^2 \leq \|\mathbf{r}_k\|^2 + 2\mu \alpha_k \mathbf{r}_k^T J_k \tilde{\mathbf{s}}^{(k)}.$$

Note that, as $\tilde{\mathbf{s}}^{(k)}$ satisfies the normal equations associated to problem (1.3), it holds $J_k^T \mathbf{r}_k = -J_k^T J_k \tilde{\mathbf{s}}^{(k)}$, so that $\mathbf{r}_k^T J_k \tilde{\mathbf{s}}^{(k)} = -\|J_k \tilde{\mathbf{s}}^{(k)}\|^2$. The *Armijo–Goldstein principle* [2, 9] sets $\mu = \frac{1}{4}$ and determines the scalar α_k as the largest number in the sequence 2^{-i} , $i = 0, 1, \dots$, for which it holds

$$\|\mathbf{r}_k\|^2 - \|\mathbf{r}(\mathbf{x}^{(k)} + \alpha_k \tilde{\mathbf{s}}^{(k)})\|^2 \geq \frac{1}{2} \alpha_k \|J_k \tilde{\mathbf{s}}^{(k)}\|^2. \quad (2.3)$$

The iteration resulting from the solution of (2.2) is defined by the following theorem.

THEOREM 2.1. *Let $\mathbf{x}^{(k)} \in \mathbb{R}^n$ and let $\tilde{\mathbf{x}}^{(k+1)} = \mathbf{x}^{(k)} + \alpha_k \tilde{\mathbf{s}}^{(k)}$ be the Gauss–Newton iteration for (1.1), where the step $\tilde{\mathbf{s}}^{(k)}$ is determined by solving (1.4) and the step length α_k by the Armijo–Goldstein principle. Then, the iteration $\mathbf{x}^{(k+1)} = \mathbf{x}^{(k)} + \alpha_k \mathbf{s}^{(k)}$ defined by (2.2) is given by*

$$\mathbf{x}^{(k+1)} = \tilde{\mathbf{x}}^{(k+1)} - V_2 V_2^T (\mathbf{x}^{(k)} - \bar{\mathbf{x}}), \quad (2.4)$$

where $\text{rank}(J_k) = r_k$ and the columns of the matrix $V_2 = [\mathbf{v}_{r_k+1}, \dots, \mathbf{v}_n]$ are orthonormal vectors in \mathbb{R}^n spanning the null space of J_k .

Proof. The proof follows the pattern of that of Theorem 3.1 in [14]. Let $U \Sigma V^T$ be the singular value decomposition of the matrix J_k . The upper-level problem in (2.2) can be expressed as

$$\|\mathbf{x}^{(k)} - \bar{\mathbf{x}} + \alpha_k \mathbf{s}\|^2 = \|V^T (\mathbf{x}^{(k)} - \bar{\mathbf{x}} + \alpha_k \mathbf{s})\|^2 = \|\alpha_k \mathbf{y} + \mathbf{z}^{(k)}\|^2,$$

with $\mathbf{y} = V^T \mathbf{s}$ and $\mathbf{z}^{(k)} = V^T (\mathbf{x}^{(k)} - \bar{\mathbf{x}})$. Replacing J_k by its SVD and setting $\mathbf{g}^{(k)} = U^T \mathbf{r}_k$, we can rewrite (2.2) as the following diagonal linear least-squares problem

$$\begin{cases} \min_{\mathbf{y} \in \mathbb{R}^n} \|\alpha_k \mathbf{y} + \mathbf{z}^{(k)}\|^2 \\ \mathbf{y} \in \{\arg \min_{\mathbf{y} \in \mathbb{R}^n} \|\Sigma \mathbf{y} + \mathbf{g}^{(k)}\|^2\}. \end{cases}$$

Solving the lower-level minimization problem uniquely determines the components $y_i = -\sigma_i^{-1} g_i^{(k)}$, $i = 1, \dots, r_k$, while the entries y_i , $i = r_k + 1, \dots, n$, are left undetermined. Their values can be found by solving the upper-level problem. From

$$\|\alpha_k \mathbf{y} + \mathbf{z}^{(k)}\|^2 = \sum_{i=1}^{r_k} \left(-\alpha_k \frac{g_i^{(k)}}{\sigma_i} + z_i^{(k)} \right)^2 + \sum_{i=r_k+1}^n \left(\alpha_k y_i + z_i^{(k)} \right)^2,$$

we obtain $y_i = -\frac{z_i^{(k)}}{\alpha_k} = -\frac{1}{\alpha_k} \mathbf{v}_i^T (\mathbf{x}^{(k)} - \bar{\mathbf{x}})$, $i = r_k + 1, \dots, n$. Then, the solution to (2.2), that is, the next approximation to the solution of (2.1), is

$$\mathbf{x}^{(k+1)} = \mathbf{x}^{(k)} + \alpha_k V \mathbf{y} = \mathbf{x}^{(k)} - \alpha_k \sum_{i=1}^{r_k} \frac{g_i^{(k)}}{\sigma_i} \mathbf{v}_i - \sum_{i=r_k+1}^n (\mathbf{v}_i^T (\mathbf{x}^{(k)} - \bar{\mathbf{x}})) \mathbf{v}_i,$$

where the last summation can be written in matrix form as $V_2 V_2^T (\mathbf{x}^{(k)} - \bar{\mathbf{x}})$, and the columns of $V_2 = [\mathbf{v}_{r_k+1}, \dots, \mathbf{v}_n]$ are a basis for $\mathcal{N}(J_k)$.

It is immediate (see [14, Theorem 3.1]) to prove that

$$\tilde{\mathbf{x}}^{(k+1)} = \mathbf{x}^{(k)} + \alpha_k \tilde{\mathbf{s}}^{(k)} = \mathbf{x}^{(k)} - \alpha_k \sum_{i=1}^{r_k} \frac{g_i^{(k)}}{\sigma_i} \mathbf{v}_i,$$

from which (2.4) follows. \square

Summarizing, the MNGN method consists of the iteration

$$\mathbf{x}^{(k+1)} = \mathbf{x}^{(k)} + \alpha_k \mathbf{s}^{(k)},$$

where the step is

$$\mathbf{s}^{(k)} = \tilde{\mathbf{s}}^{(k)} - \frac{1}{\alpha_k} \mathbf{t}^{(k)},$$

with

$$\tilde{\mathbf{s}}^{(k)} = - \sum_{i=1}^{r_k} \frac{g_i^{(k)}}{\sigma_i} \mathbf{v}_i, \quad \mathbf{t}^{(k)} = V_2 V_2^T (\mathbf{x}^{(k)} - \bar{\mathbf{x}}). \quad (2.5)$$

Since $\mathcal{P}_{\mathcal{N}(J_k)} = V_2 V_2^T$ is the orthogonal projector onto $\mathcal{N}(J_k)$, the above theorem states that the $(k+1)$ th iterate of the MNGN method is orthogonal to the null space of J_k .

Theorem 2.1 shows that the correction vector $\mathbf{t}^{(k)}$ defined in (2.5), which allows to compute the minimal-norm solution at each step, is not damped by the parameter α_k . As a result, in some numerical examples the method fails to converge, because projecting the solution orthogonally to the null space of J_k causes the residual to increase. To understand how this can happen, a second-order analysis of the objective function is required.

The second-order Taylor approximation to the function $f(\mathbf{x}) = \frac{1}{2} \|\mathbf{r}(\mathbf{x})\|^2$ at $\mathbf{x}^{(k+1)} = \mathbf{x}^{(k)} + \alpha \mathbf{s}$ is

$$f(\mathbf{x}^{(k+1)}) \simeq f(\mathbf{x}^{(k)}) + \alpha \nabla f(\mathbf{x}^{(k)})^T \mathbf{s} + \frac{1}{2} \alpha^2 \mathbf{s}^T \nabla^2 f(\mathbf{x}^{(k)}) \mathbf{s}. \quad (2.6)$$

The gradient and the Hessian of $f(\mathbf{x})$, written in matrix form, are given by

$$\nabla f(\mathbf{x}) = J(\mathbf{x})^T \mathbf{r}(\mathbf{x}), \quad \nabla^2 f(\mathbf{x}) = J(\mathbf{x})^T J(\mathbf{x}) + \mathcal{Q}(\mathbf{x}),$$

where

$$\mathcal{Q}(\mathbf{x}) = \sum_{i=1}^m r_i(\mathbf{x}) \nabla^2 r_i(\mathbf{x}),$$

and $\nabla^2 r_i(\mathbf{x})$ is the Hessian matrix of $r_i(\mathbf{x})$. By replacing the expression of f and $\alpha \mathbf{s} = \alpha \tilde{\mathbf{s}} - \mathbf{t}$ in (2.6), where $\tilde{\mathbf{s}}$ is the Gauss–Newton step and \mathbf{t} is in the null space of J_k , and letting $\mathcal{Q}_k = \mathcal{Q}(\mathbf{x}^{(k)})$, the following approximation is obtained

$$\begin{aligned} \frac{1}{2} \|\mathbf{r}_{k+1}\|^2 &\simeq \frac{1}{2} \|\mathbf{r}_k\|^2 + \alpha \mathbf{r}_k^T J_k \mathbf{s} + \frac{1}{2} \alpha^2 \mathbf{s}^T (J_k^T J_k + \mathcal{Q}_k) \mathbf{s} \\ &= \frac{1}{2} \|\mathbf{r}_k\|^2 + \alpha \mathbf{r}_k^T J_k \tilde{\mathbf{s}} + \frac{1}{2} \alpha^2 \tilde{\mathbf{s}}^T (J_k^T J_k + \mathcal{Q}_k) \tilde{\mathbf{s}} - \alpha \mathbf{t}^T \mathcal{Q}_k \tilde{\mathbf{s}} + \frac{1}{2} \mathbf{t}^T \mathcal{Q}_k \mathbf{t}. \end{aligned}$$

The first two terms containing second derivatives (the matrix \mathcal{Q}_k) are damped by the α parameter. If the function F is mildly nonlinear, the third term $\frac{1}{2} \mathbf{t}^T \mathcal{Q}_k \mathbf{t}$ is negligible. In the presence of a strong nonlinearity, its contribution to the residual is significant and may lead to its growth. This shows that a damping parameter is required to control the step length for both the Gauss–Newton step $\tilde{\mathbf{s}}$ and the correction vector \mathbf{t} . If a relaxation parameter is introduced for \mathbf{t} , Theorem 2.1 implies that the minimal-norm solution of (2.2) can only be approximated.

REMARK 2.2. We report a simple low dimensional example for which the MNGN method may not converge. Let us consider the function $F : \mathbb{R}^2 \rightarrow \mathbb{R}$ defined by

$$F(\mathbf{x}) = \delta^2 [(x_1 - \gamma)^2 + (x_2 - \gamma)^2] - 1,$$

depending on the parameters $\delta, \gamma \in \mathbb{R}$. Since the Hessian matrix of the residual is given by

$$\nabla^2 r(\mathbf{x}) = \begin{bmatrix} 2\delta^2 & 0 \\ 0 & 2\delta^2 \end{bmatrix},$$

the second-order term $\frac{1}{2} \mathbf{t}^T \mathcal{Q}_k \mathbf{t}$ is not negligible, in general, when δ is large.

3. Estimating the rank of the Jacobian. In order to apply Theorem 2.1 to computing the minimal-norm solution by (2.4), the rank of the Jacobian matrix $J_k = J(\mathbf{x}^{(k)})$ should be known in advance. As the rank may vary along the iterations, we set $r_k = \text{rank}(J_k)$. The knowledge of r_k for each $k = 0, 1, \dots$, is not generally available, making it necessary to estimate its value at each iteration step, to avoid nonconvergence or a breakdown of the algorithm.

In such situations, it is common to consider the numerical rank $r_{\epsilon,k}$ of J_k , sometimes denoted as ϵ -rank, where ϵ represents a chosen tolerance. The numerical rank is defined in terms of the singular values $\sigma_i^{(k)}$ of J_k , as the integer $r_{\epsilon,k}$ such that

$$\sigma_{r_{\epsilon,k}}^{(k)} > \epsilon \geq \sigma_{r_{\epsilon,k}+1}^{(k)}.$$

Theorem 2.1 can be adapted to this setting, by simply replacing at each iteration the rank r_k with the numerical rank $r_{\epsilon,k}$.

Determining the numerical rank is a difficult task for discrete ill-posed problems, in which the singular values decay monotonically to zero. In such a case, the numerical rank plays the role of a regularization parameter and is estimated by suitable methods, which often require information about the noise level and type; see, e.g., [11, 15].

When the problem is locally rank-deficient, meaning that the rank of $J(\mathbf{x})$ depends on the evaluation vector \mathbf{x} , the numerical rank $r_{\epsilon,k}$ can be determined, in principle, by choosing a suitable value of ϵ . Numerical experiments show that a fixed value of ϵ does not always lead to a correct estimation of $r_{\epsilon,k}$, and that it is preferable to determine the ϵ -rank by searching for a sensible gap between $\sigma_{r_{\epsilon,k}}^{(k)}$ and $\sigma_{r_{\epsilon,k}+1}^{(k)}$.

To locate such a gap, we adopt a heuristic approach already applied in [4] for the same purpose, in a different setting. At each step, we compute the ratios

$$\rho_i^{(k)} = \frac{\sigma_i^{(k)}}{\sigma_{i+1}^{(k)}}, \quad i = 1, 2, \dots, q-1,$$

where $q = \min(m, n)$. Then, we consider the index set

$$\mathcal{I}_k = \left\{ i \in \{1, 2, \dots, q-1\} : \rho_i^{(k)} > R \text{ and } \sigma_i^{(k)} > \tau \right\}.$$

In our numerical simulations, we set $R = 10^2$ and $\tau = 10^{-8}$. An index i belongs to \mathcal{I}_k if there is a significant “jump” between $\sigma_i^{(k)}$ and $\sigma_{i+1}^{(k)}$, and $\sigma_i^{(k)}$ is numerically nonzero. If the set \mathcal{I}_k is empty, we set $r_{\epsilon,k} = q$. Otherwise, we consider

$$\rho_j^{(k)} = \max_{i \in \mathcal{I}_k} \rho_i^{(k)}, \quad (3.1)$$

and we define $r_{\epsilon,k} = j$. This amounts to selecting the largest gap between “large” and “small” singular values.

4. Choosing the projection step length. The occasional nonconvergence in the computation of the minimal-norm solution to a nonlinear least-squares problem was discussed in [3], where the authors propose an iterative method based on a convex combination of the Gauss–Newton and the minimal-norm Gauss–Newton iterates. Following our notation, it can be expressed in the form

$$\mathbf{x}^{(k+1)} = (1 - \gamma_k) \left[\mathbf{x}^{(k)} + \tilde{\mathbf{s}}^{(k)} \right] + \gamma_k \left[\mathbf{x}^{(k)} + \tilde{\mathbf{s}}^{(k)} - V_2 V_2^T \mathbf{x}^{(k)} \right], \quad (4.1)$$

where the parameters $\gamma_k \in [0, 1]$, for $k = 0, 1, \dots$, form a sequence converging to zero. The standard Gauss–Newton method is obtained by setting $\gamma_k = 0$, while $\gamma_k = 1$ leads to the minimal-norm Gauss–Newton method. In their numerical examples, the authors adopt the sequences $\gamma_k = (0.5)^{k+1}$ and $\gamma_k = (0.5)^{2^k}$.

It is immediate to rewrite (4.1) in the form (1.8), showing that the method proposed in [3] is equivalent to the application of the undamped Gauss–Newton method, whose convergence is not theoretically guaranteed [2], with a damped correction to favor the decrease of the norm of the solution. The numerical experiments reported in the paper show that the minimization of the residual is sped up if γ_k quickly converges to zero, while the norm of the solution decreases faster if γ_k has a slower decay. The choice of the sequence of parameters appears to be critical to tune the performance of the algorithm, and no adaptive choice for γ_k is proposed.

In this paper, we propose to introduce a second relaxation parameter, β_k , to control the step length of the minimal-norm correction $\mathbf{t}^{(k)}$ defined in (2.5). The new iterative method is denoted by MNGN2 and it takes the form

$$\mathbf{x}^{(k+1)} = \mathbf{x}^{(k)} + \alpha_k \tilde{\mathbf{s}}^{(k)} - \beta_k \mathbf{t}^{(k)}, \quad (4.2)$$

where $\tilde{\mathbf{s}}^{(k)}$ is the step vector produced by the Gauss–Newton method and $\mathbf{t}^{(k)}$ is the projection vector which makes the norm of $\mathbf{x}^{(k+1)}$ minimal, without changing the value of the linearized residual.

The second-order analysis reported at the end of Section 2 may be adapted for the CKB method (1.8). It shows that neither the CKB nor the MNGN method are guaranteed to converge, as both the Gauss–Newton search direction and the projection step should be damped to ensure that the residual decreases. The MNGN2 method locally converges if α_k and β_k are suitably chosen, but it will recover the minimal-norm solution only if $\beta_k \simeq 1$ for k close to convergence.

Our numerical tests showed that it is important to choose both α_k and β_k adaptively along the iterations. A simple solution is to let $\beta_k = \alpha_k$ and estimate α_k by the Armijo–Goldstein principle (2.3), with $\mathbf{s}^{(k)} = \tilde{\mathbf{s}}^{(k)} - \mathbf{t}^{(k)}$ in place of $\tilde{\mathbf{s}}^{(k)}$. This approach proves to be effective in the computation of the minimal-norm solution, but its convergence is often rather slow. To speed up iteration we propose a procedure to adaptively choose the value of β_k .

Algorithm 1 Outline of the MNGN2 method.

Require: nonlinear function F , data vector \mathbf{b} ,
Require: initial solution $\mathbf{x}^{(0)}$, model profile $\bar{\mathbf{x}}$, tolerance η for residual increase
Ensure: approximation $\mathbf{x}^{(k+1)}$ of minimal-norm least-squares solution

- 1: $k = 0, \beta = 1$
- 2: **repeat**
- 3: $k = k + 1$
- 4: estimate $r_k = \text{rank}(J(\mathbf{x}^{(k)}))$ by (3.1)
- 5: compute $\tilde{\mathbf{s}}^{(k)}$ by the Gauss–Newton method (1.3)
- 6: compute α_k by the Armijo–Goldstein principle (2.3)
- 7: compute $\mathbf{t}^{(k)}$ by (2.5)
- 8: **if** $\beta < 1$ **then**
- 9: $\beta = 2\beta$
- 10: **end if**
- 11: $\tilde{\mathbf{x}}^{(k+1)} = \mathbf{x}^{(k)} + \alpha_k \tilde{\mathbf{s}}^{(k)}$
- 12: $\tilde{\rho}_{k+1} = \|F(\tilde{\mathbf{x}}^{(k+1)}) - \mathbf{b}\| + \varepsilon_M$
- 13: $\mathbf{x}^{(k+1)} = \tilde{\mathbf{x}}^{(k+1)} - \beta \mathbf{t}^{(k)}$
- 14: $\rho_{k+1} = \|F(\mathbf{x}^{(k+1)}) - \mathbf{b}\|$
- 15: **while** $(\rho_{k+1} > \tilde{\rho}_{k+1} + \delta(\tilde{\rho}_{k+1}, \eta))$ **and** $(\beta > 10^{-8})$ **do**
- 16: $\beta = \beta/2$
- 17: $\mathbf{x}^{(k+1)} = \tilde{\mathbf{x}}^{(k+1)} - \beta \mathbf{t}^{(k)}$
- 18: $\rho_{k+1} = \|F(\mathbf{x}^{(k+1)}) - \mathbf{b}\|$
- 19: **end while**
- 20: $\beta_k = \beta$
- 21: **until** convergence

This procedure is outlined in Algorithm 1. Initially, we set $\beta = 1$. At each iteration, we compute the residual at the Gauss–Newton iteration $\tilde{\mathbf{x}}^{(k+1)}$ and at the

tentative iteration $\mathbf{x}^{(k+1)} = \tilde{\mathbf{x}}^{(k+1)} - \beta \mathbf{t}^{(k)}$. Subtracting the vector $\beta \mathbf{t}^{(k)}$ may cause the residual to increase. We accept such an increase if

$$\|\mathbf{r}(\mathbf{x}^{(k+1)})\| \leq \|\mathbf{r}(\tilde{\mathbf{x}}^{(k+1)})\| + \delta(\|\mathbf{r}(\tilde{\mathbf{x}}^{(k+1)})\|, \eta), \quad (4.3)$$

where $\delta(\rho, \eta)$ is a function determining the maximal increase allowed in the residual $\rho = \|\mathbf{r}(\tilde{\mathbf{x}}^{(k+1)})\|$, and $\eta > 0$ is a chosen tolerance. On the contrary, β is halved and the residual is recomputed until (4.3) is verified or β becomes excessively small. To allow β to increase, we tentatively double it at each iteration (see line 9 in the algorithm) before applying the above procedure. At line 12 of the algorithm we add the machine epsilon ε_M to the actual residual $\tilde{\rho}_{k+1}$ to avoid that $\delta(\tilde{\rho}_{k+1}, \eta)$ becomes zero.

A possible choice for the value of the residual increase is $\delta(\rho, \eta) = \eta \rho$, with η suitably chosen. Our experiments showed that it is possible to find, by chance, a value of η which produces good results, but its choice is strongly dependent on the particular example. We also noticed that, in cases where the residual stagnates, accepting a large increase in the residual may lead to nonconvergence. In such situations, a fixed multiple of the residual is not well suited to model its increase. Indeed, if the residual is large, one is prone to accept only a small increase, while if the residual is very small, a relatively large growth may be acceptable.

To overcome these difficulties, we consider $\delta(\rho, \eta) = \rho^\eta$, and choose η at each step by the adaptive procedure described in Algorithm 2. When at least k_{res} iterations have been performed, we compute the linear polynomial which fits the logarithm of the last k_{res} residuals in the least-squares sense. To detect if the residual stagnates or increases, we check if the slope M of the regression line exceeds -10^{-2} . If this happens, the value of η is doubled. The effect on the algorithm is to enhance the importance of the decrease of the residual and reduce that of the norm. To recover a sensible decrease in the norm, if at a subsequent step the residual reduction accelerates (e.g., $M < -\frac{1}{2}$), the value of η is halved. In our experiments, we initialize η to $\frac{1}{8}$ and set $k_{\text{res}} = 5$.

REMARK 4.1. The adaptive estimation of $\delta(\rho, \eta)$ does not significantly increase the complexity of Algorithm 1, as line 3 of Algorithm 2 implies the solution of a 2×2 linear system whose matrix is fixed and can be computed in advance, while forming the right-hand side requires $4k_{\text{res}}$ floating point operations.

Algorithm 2 Adaptive determination of the residual increase $\delta(\rho, \eta)$.

Require: actual residual $\rho = \|\mathbf{r}(\tilde{\mathbf{x}}^{(k+1)})\|$, starting tolerance η
Require: iteration index k , residuals $\theta_j = \|\mathbf{r}(\tilde{\mathbf{x}}^{(k-k_{\text{res}}+j)})\|$, $j = 1, \dots, k_{\text{res}}$
Ensure: residual increase $\delta(\rho, \eta)$

- 1: $M_{\min} = -10^{-2}$, $M_{\max} = -\frac{1}{2}$
- 2: **if** $k \geq k_{\text{res}}$ **then**
- 3: compute regression line $p_1(t) = Mt + N$ of $(j, \log(\theta_j))$, $j = 1, \dots, k_{\text{res}}$
- 4: **if** $M > M_{\min}$ **then**
- 5: $\eta = 2\eta$
- 6: **else if** $M < M_{\max}$ **then**
- 7: $\eta = \eta/2$
- 8: **end if**
- 9: **end if**
- 10: $\delta(\rho, \eta) = \rho^\eta$

To detect convergence, we interrupt the iteration as soon as

$$\|\mathbf{x}^{(k+1)} - \mathbf{x}^{(k)}\| < \tau \|\mathbf{x}^{(k+1)}\| \quad \text{or} \quad \|\alpha_k \tilde{\mathbf{s}}^{(k)}\| < \tau, \quad (4.4)$$

or when a fixed number of iteration N_{\max} is exceeded. The second stop condition in (4.4) detects the slow progress of the relaxed Gauss–Newton iteration algorithm. This often happens close to the solution. The stop tolerance is set to $\tau = 10^{-8}$.

5. Nonlinear minimal- L -norm solution. The introduction of a regularization matrix $L \in \mathbb{R}^{p \times n}$, $p \leq n$, in least-squares problems was originally connected to the numerical treatment of linear discrete ill-posed problems, and in particular to Tikhonov regularization. The use of a regularization matrix is also justified in under-determined least-squares problems to select a solution with particular features, such as smoothness or sparsity, among the infinitely many possible solutions.

While in (1.6) the seminorm $\|L\mathbf{s}\|$ is minimized over all the updating vectors \mathbf{s} which minimize the linearized residual, here we seek to compute the minimal- L -norm solution to the nonlinear problem (1.1), that is the vector \mathbf{x} which solves the constrained problem

$$\begin{cases} \min_{\mathbf{x} \in \mathbb{R}^n} \|L(\mathbf{x} - \bar{\mathbf{x}})\|^2 \\ \mathbf{x} \in \{\arg \min_{\mathbf{x} \in \mathbb{R}^n} \|F(\mathbf{x}) - \mathbf{b}\|^2\}. \end{cases} \quad (5.1)$$

Similarly to Section 2, we consider an iterative method of the type (1.2), where the step $\mathbf{s}^{(k)}$ is the solution of the linearized problem

$$\begin{cases} \min_{\mathbf{s} \in \mathbb{R}^n} \|L(\mathbf{x}^{(k)} - \bar{\mathbf{x}} + \alpha \mathbf{s})\|^2 \\ \mathbf{s} \in \{\arg \min_{\mathbf{s} \in \mathbb{R}^n} \|J_k \mathbf{s} + \mathbf{r}_k\|^2\}. \end{cases} \quad (5.2)$$

We will denote the iteration resulting from the solution of (5.2) as the *minimal- L -norm Gauss–Newton* (MLNGN) method.

We recall the definition of the generalized singular value decomposition (GSVD) of a matrix pair (J, L) [10]. Let $J \in \mathbb{R}^{m \times n}$ and $L \in \mathbb{R}^{p \times n}$ be matrices with $\text{rank}(J) = r$ and $\text{rank}(L) = p$. Assume that $m + p \geq n$ and

$$\text{rank} \left(\begin{bmatrix} J \\ L \end{bmatrix} \right) = n,$$

which corresponds to requiring that $\mathcal{N}(J) \cap \mathcal{N}(L) = \{0\}$. The GSVD of the matrix pair (J, L) is defined as the factorization

$$J = U \Sigma_J W^{-1}, \quad L = V \Sigma_L W^{-1},$$

where $U \in \mathbb{R}^{m \times m}$ and $V \in \mathbb{R}^{p \times p}$ are matrices with orthonormal columns \mathbf{u}_i and \mathbf{v}_i , respectively, and $W \in \mathbb{R}^{n \times n}$ is nonsingular. If $m \geq n \geq r$, the matrices $\Sigma_J \in \mathbb{R}^{m \times n}$ and $\Sigma_L \in \mathbb{R}^{p \times n}$ have the form

$$\Sigma_J = \left[\begin{array}{c} O_{n-r} \\ \hline C \\ \hline I_d \\ O_{(m-n) \times n} \end{array} \right], \quad \Sigma_L = \left[\begin{array}{c|c} I_{p-r+d} & \\ \hline & S \end{array} \right] O_{p \times d},$$

where $d = n - p$,

$$\begin{aligned} C &= \text{diag}(c_1, \dots, c_{r-d}), & 0 < c_1 \leq c_2 \leq \dots \leq c_{r-d} < 1, \\ S &= \text{diag}(s_1, \dots, s_{r-d}), & 1 > s_1 \geq s_2 \geq \dots \geq s_{r-d} > 0, \end{aligned} \quad (5.3)$$

with $c_i^2 + s_i^2 = 1$, for $i = 1, \dots, r-d$. The identity matrix of size k is denoted by I_k , while O_k and $O_{k \times \ell}$ are zero matrices of size k and $k \times \ell$, respectively; a matrix block has to be omitted when one of its dimensions is zero. The scalars $\gamma_i = \frac{c_i}{s_i}$ are called *generalized singular values*, and they appear in nondecreasing order.

If $r \leq m < n$, the matrices $\Sigma_J \in \mathbb{R}^{m \times n}$ and $\Sigma_L \in \mathbb{R}^{p \times n}$ take the form

$$\Sigma_J = \left[\begin{array}{c|cc} O_{m \times (n-m)} & O_{m-r} & C \\ & C & I_d \end{array} \right], \quad \Sigma_L = \left[\begin{array}{c|c} I_{p-r+d} & O_{p \times d} \\ S & \end{array} \right],$$

where the blocks are defined as above.

Let $J_k = U \Sigma_J W^{-1}$, $L = V \Sigma_L W^{-1}$ be the GSVD of the matrix pair (J_k, L) . We indicate by \mathbf{w}_i the column vectors of the matrix W , and by $\widehat{\mathbf{w}}^j$ the rows of W^{-1} , that is

$$W = [\mathbf{w}_1, \dots, \mathbf{w}_n], \quad W^{-1} = \begin{bmatrix} \widehat{\mathbf{w}}^1 \\ \vdots \\ \widehat{\mathbf{w}}^n \end{bmatrix}.$$

We have $\mathcal{N}(J_k) = \text{span}(\mathbf{w}_1, \dots, \mathbf{w}_{n-r_k})$, if $r_k = \text{rank}(J_k)$; see [14] for a proof.

THEOREM 5.1. *Let $\mathbf{x}^{(k)} \in \mathbb{R}^n$ and let $\tilde{\mathbf{x}}^{(k+1)} = \mathbf{x}^{(k)} + \alpha_k \tilde{\mathbf{s}}^{(k)}$ be the Gauss–Newton iteration for (1.1), where the step $\tilde{\mathbf{s}}^{(k)}$ is determined by solving (1.6) and the step length α_k by the Armijo–Goldstein principle. Then, the iteration $\mathbf{x}^{(k+1)} = \mathbf{x}^{(k)} + \alpha_k \mathbf{s}^{(k)}$ for (5.2), is given by*

$$\mathbf{x}^{(k+1)} = \tilde{\mathbf{x}}^{(k+1)} - W_1 \widehat{W}_1 (\mathbf{x}^{(k)} - \bar{\mathbf{x}}), \quad (5.4)$$

where $\widehat{W}_1 \in \mathbb{R}^{(n-r_k) \times n}$ contains the first $n - r_k$ rows of W^{-1} , and $W_1 \in \mathbb{R}^{n \times (n-r_k)}$ is composed of the first $n - r_k$ columns of W .

Proof. The proof proceeds analogously to that of Theorem 4.2 in [14]. Replacing J_k and L with their GSVD and setting $\mathbf{y} = W^{-1} \mathbf{s}$, $\mathbf{z}^{(k)} = W^{-1} (\mathbf{x}^{(k)} - \bar{\mathbf{x}})$, and $\mathbf{g}^{(k)} = U^T \mathbf{r}_k$, (5.2) can be rewritten as the following diagonal least-squares problem

$$\begin{cases} \min_{\mathbf{y} \in \mathbb{R}^n} \|\Sigma_L(\alpha_k \mathbf{y} + \mathbf{z}^{(k)})\|^2 \\ \mathbf{y} \in \{\arg \min_{\mathbf{y} \in \mathbb{R}^n} \|\Sigma_J \mathbf{y} + \mathbf{g}^{(k)}\|^2\}. \end{cases}$$

When $m \geq n$, the diagonal linear system in the constraint is solved by a vector \mathbf{y} with entries

$$y_i = \begin{cases} -\frac{g_i^{(k)}}{c_{i-n+r_k}}, & i = n - r_k + 1, \dots, p, \\ -g_i^{(k)}, & i = p + 1, \dots, n. \end{cases}$$

The components y_i , for $i = 1, \dots, n - r_k$, can be determined by minimizing the norm

$$\begin{aligned} \|\Sigma_L(\alpha_k \mathbf{y} + \mathbf{z}^{(k)})\|^2 &= \sum_{i=1}^{n-r_k} \left(\alpha_k y_i + z_i^{(k)} \right)^2 \\ &+ \sum_{i=n-r_k+1}^p \left(-\alpha_k \frac{g_i^{(k)}}{\gamma_{i-n+r_k}} + s_{i-n+r_k} z_i^{(k)} \right)^2, \end{aligned} \quad (5.5)$$

where $\gamma_i = \frac{c_i}{s_i}$ are the generalized singular values of the matrix pair (J_k, L) . The minimum of (5.5) is reached for $y_i = -\frac{1}{\alpha_k} z_i^{(k)} = -\frac{1}{\alpha_k} \widehat{\mathbf{W}}^i(\mathbf{x}^{(k)} - \bar{\mathbf{x}})$, $i = 1, \dots, n - r_k$, and the solution to (5.2), that is, the next approximation to the solution of (5.1), is

$$\begin{aligned} \mathbf{x}^{(k+1)} &= \mathbf{x}^{(k)} + \alpha_k W \mathbf{y} \\ &= \mathbf{x}^{(k)} - \sum_{i=1}^{n-r_k} z_i^{(k)} \mathbf{w}_i - \alpha_k \sum_{i=n-r_k+1}^p \frac{g_i^{(k)}}{c_{i-n+r_k}} \mathbf{w}_i - \alpha_k \sum_{i=p+1}^n g_i^{(k)} \mathbf{w}_i, \end{aligned} \quad (5.6)$$

where the first summation in the right-hand side can be rewritten as $W_1 \widehat{W}_1(\mathbf{x}^{(k)} - \bar{\mathbf{x}})$. Applying the same procedure to (1.6), we obtain

$$\tilde{\mathbf{x}}^{(k+1)} = \mathbf{x}^{(k)} - \alpha_k \sum_{i=n-r_k+1}^p \frac{g_i^{(k)}}{c_{i-n+r_k}} \mathbf{w}_i - \alpha_k \sum_{i=p+1}^n g_i^{(k)} \mathbf{w}_i,$$

from which (5.4) follows. Since solving (5.2) for $m < n$ leads to a formula similar to (5.6), with $g_{i-n+m}^{(k)}$ in place of $g_i^{(k)}$, the validity of (5.4) is confirmed. \square

As in the computation of the minimal-norm solution, the iteration based on (5.4) fails to converge without a suitable relaxation parameter β_k for the projection vector $\mathbf{t}^{(k)} = W_1 \widehat{W}_1(\mathbf{x}^{(k)} - \bar{\mathbf{x}})$. We adopted an iteration similar to (4.2), choosing β_k by adapting Algorithms 1 and 2 to this setting. It is important to note that $\tilde{\mathcal{P}}_{\mathcal{N}(J_k)} = W_1 \widehat{W}_1$ is an oblique projector onto $\mathcal{N}(J_k)$.

At the same time, the rank of the Jacobian is estimated at each step by applying the procedure described in Section 3 to the diagonal elements $c_j^{(k)}$, $j = 1, \dots, q - d$, of the GSVD factor Σ_J of J_k ; see (5.3). In this case, at each step, we compute the ratios

$$\rho_i^{(k)} = \frac{c_{i+1}^{(k)}}{c_i^{(k)}}, \quad i = 1, 2, \dots, q - d - 1,$$

where $q = \min(m, n)$.

Actually, the GSVD routine computes the matrix W^{-1} , but the matrix W is needed for the computation of both the vectors $\tilde{\mathbf{s}}^{(k)}$ and $\mathbf{t}^{(k)}$. To reduce the computational load, we compute at each iteration the LU factorization $PW^{-1} = LU$, and we use it to solve the linear system with two right-hand sides

$$W^{-1} \begin{bmatrix} \mathbf{t}^{(k)} & \tilde{\mathbf{s}}^{(k)} \end{bmatrix} = \begin{bmatrix} \widehat{W}_1(\mathbf{x}^{(k)} - \bar{\mathbf{x}}) & \mathbf{0}_{n-r} \\ \mathbf{0}_r & \tilde{\mathbf{y}} \end{bmatrix},$$

where $\tilde{\mathbf{y}} \in \mathbb{R}^r$ contains the last r components of the vector \mathbf{y} appearing in (5.6), and $\mathbf{0}_k$ denotes the zero vector of size k .

6. Test problems and numerical results. The MNGN2 method, defined by (4.2), was implemented in the Matlab programming language; the software is available from the authors. The developed functions implement all the variants of the MNGN2 algorithm, as well as the MNGN and CKB methods developed in [14] and [3], respectively. To compare the methods and investigate their performance, we performed numerical experiments on various test problems that highlight particular difficulties in the computation of the minimal-norm solution.

For each experiment, we repeated the computation 100 times, varying the starting point $\mathbf{x}^{(0)}$ by letting its components be uniformly distributed random numbers in $[-5, 5]$. The model profile $\bar{\mathbf{x}}$ was set to the zero vector, except where indicated.

We consider a numerical test a “success” if the algorithm converges according to condition (4.4), with stop tolerance $\tau = 10^{-8}$ and maximum number of iterations $N_{\max} = 500$. A failure is not a serious problem, in general, because nonconvergence simply suggests to try a different starting vector. Anyway, if this happens too often, it increases the computational load. At the same time, a success of a method does not imply that it recovers the minimal-norm solution, as the convergence is only local. So, to give an idea of the performance of the methods, we measure over all the tests the average of both the number of iterations required and the norm of the converged solution $\|\tilde{\mathbf{x}}\|$. We also report the number of successes.

In the following, the MNGN2 algorithm (4.2) will be denoted by different names, according to the particular implementation. In the method denoted by MNGN2_α , we let $\beta_k = \alpha_k$ in (4.2), and determine α_k by the Armijo–Goldstein principle. Algorithm 1 is denoted by $\text{MNGN2}_{\alpha\beta}$, when $\delta(\rho, \eta) = \eta\rho$, with a fixed value of η . The same algorithm with $\delta(\rho, \eta) = \rho^\eta$, and η estimated by Algorithm 2, is labeled as $\text{MNGN2}_{\alpha\beta\delta}$. The algorithm (4.1) developed in [3] is denoted by CKB_1 when $\gamma_k = (0.5)^{k+1}$, and by CKB_2 when $\gamma_k = (0.5)^{2^k}$. The same algorithms are denoted by rCKB_1 and rCKB_2 when they are applied with the automatic estimation of the rank of the Jacobian, discussed in Section 3.

We note that the computational cost of each iteration is roughly the same for all the methods considered. Indeed, the additional complexity required by the MNGN2 algorithms consists of the estimation of the numerical rank $r_{\epsilon, k}$, of the residual increase $\delta(\rho, \eta)$, and of the projection parameter β_k . All these computations involve a small number of floating point operations; see also Remark 4.1.

EXAMPLE 6.1.

In this first example we consider a nonlinear model that describes the behaviour of a redundant parallel robot. It is a problem that concerns the inverse kinematics of position, and is defined by the following function $F : \mathbb{R}^4 \rightarrow \mathbb{R}^2$

$$F(\mathbf{x}) = \begin{bmatrix} (X - A \cos(x_1))^2 + (Y - A \sin(x_1))^2 - x_2^2 \\ (X - A \cos(x_3) - H)^2 + (Y - A \sin(x_3))^2 - x_4^2 \end{bmatrix},$$

with the data vector $\mathbf{b} = \mathbf{0}$ in (1.1). The model describes the kinematic of a robotic arm moved by 4 motors, whose position is identified by the unknowns $\{x_i\}_{i=1}^4$, which must reach a point with given coordinates (X, Y) ; A and H are parameters describing the system. In our simulation we assume $(X, Y) = (3, 3)$, $A = 2$, $H = 10$.

The Jacobian matrix of F is

$$J(\mathbf{x}) = \begin{bmatrix} \frac{\partial F_1}{\partial x_1} & \frac{\partial F_1}{\partial x_2} & 0 & 0 \\ 0 & 0 & \frac{\partial F_2}{\partial x_3} & \frac{\partial F_2}{\partial x_4} \end{bmatrix},$$

with

$$\begin{aligned}\frac{\partial F_1}{\partial x_1} &= 2A(X - A \cos(x_1)) \sin(x_1) - 2A(Y - A \sin(x_1)) \cos(x_1), \\ \frac{\partial F_2}{\partial x_3} &= 2A(X - A \cos(x_3) - H) \sin(x_3) - 2A(Y - A \sin(x_3)) \cos(x_3), \\ \frac{\partial F_1}{\partial x_2} &= -2x_2, \quad \frac{\partial F_2}{\partial x_4} = -2x_4.\end{aligned}$$

The results obtained are reported in Table 6.1. We see that the MNGN2_α and CKB_1 methods recover solutions with smaller norms, in the average, but the first one requires a large number of iterations. The $\text{MNGN2}_{\alpha\beta\delta}$ implementation, with automatic estimation of the projection step β_k , quickly converges but produces solutions with slightly larger norms. The CKB_2 method leads to solutions with a worse norm, testifying that the performance of the method in (4.1) is very sensitive to the choice of the sequence γ_k . The MNGN method from [14] leads to solutions far from optimality, and fails in 70% of the tests. This happens in most of the examples considered in this paper, so we will involve it only in another experiment.

TABLE 6.1
Results for Example 6.1.

method	iterations	$\ \tilde{\mathbf{x}}\ $	#success
MNGN2_α	239	8.7246	92
$\text{MNGN2}_{\alpha\beta\delta}$	38	9.0621	96
CKB_1	26	8.5515	100
CKB_2	10	9.7344	100
MNGN	182	17.6329	30

EXAMPLE 6.2.

Here we consider a test problem introduced in [3]. Let $F : \mathbb{R}^3 \rightarrow \mathbb{R}$ be the nonlinear function defined by

$$F(\mathbf{x}) = x_3 - (x_1 - 1)^2 - 2(x_2 - 2)^2 - 3.$$

The equation $F(\mathbf{x}) = 0$ represents an elliptic paraboloid in \mathbb{R}^3 with vertex $\mathbf{V} = (1, 2, 3)^T$. We remark that the minimal-norm solution is the point

$$\mathbf{x}^* \approx (0.859754, 1.849178, 3.065164)^T,$$

and not the vector $\hat{\mathbf{x}}$ reported in [3, Sec. 4.2]. Indeed, $\|\mathbf{x}^*\| \approx 3.681558$, whereas $\|\hat{\mathbf{x}}\| \approx 3.706359$.

The results obtained are reported in Table 6.2. The $\text{MNGN2}_{\alpha\beta}$ method is tested with two values of the parameter η appearing in the residual increase $\delta(\rho, \eta) = \eta\rho$; see Algorithm 1. It is clear that it can lead to accurate solutions only if the parameter is suitably chosen ($\eta = 2$). On the contrary ($\eta = 8$), it shows a great number of failures.

As in the previous example, the best results are produced by MNGN2_α , and $\text{MNGN2}_{\alpha\beta\delta}$ reaches very similar solutions but is about 10 times faster. The CKB methods take a smaller number of iterations, but produce less accurate solutions.

EXAMPLE 6.3.

Let $F : \mathbb{R}^n \rightarrow \mathbb{R}^m$ be the nonlinear function

$$F(\mathbf{x}) = [F_1(\mathbf{x}), F_2(\mathbf{x}), \dots, F_m(\mathbf{x})]^T, \quad m \leq n, \quad (6.1)$$

TABLE 6.2
Results for Example 6.2.

method	iterations	$\ \tilde{\mathbf{x}}\ $	#success
MNGN2 $_{\alpha\beta}$ ($\eta = 8$)	174	3.6903	15
MNGN2 $_{\alpha\beta}$ ($\eta = 2$)	62	3.7120	100
MNGN2 $_{\alpha}$	330	3.6816	100
MNGN2 $_{\alpha\beta\delta}$	37	3.6832	100
CKB $_1$	26	3.7343	100
CKB $_2$	10	3.7561	100

defined by

$$F_i(\mathbf{x}) = \frac{1}{2}S(\mathbf{x}) (x_i^2 + 1), \quad i = 1, \dots, m,$$

where

$$S(\mathbf{x}) = \sum_{j=1}^n \left(\frac{x_j - c_j}{a_j} \right)^2 - 1$$

is the n -ellipsoid with center $\mathbf{c} = (c_1, \dots, c_n)^T$ and whose semiaxes are the components of the vector $\mathbf{a} = (a_1, \dots, a_n)^T$. The locus of the solutions is the n -ellipsoid.

Setting $y_i = x_i^2 + 1$, for $i = 1, \dots, m$, and $z_j = \frac{x_j - c_j}{a_j^2}$, for $j = 1, \dots, n$, the Jacobian matrix can be expressed as

$$J(\mathbf{x}) = S(\mathbf{x})D_{m,n}(\mathbf{x}) + \mathbf{y}\mathbf{z}^T,$$

where $D_{m,n}(\mathbf{x})$ is an $m \times n$ diagonal matrix whose main diagonal consists of the vector \mathbf{x} . Indeed,

$$\frac{\partial F_i}{\partial x_k} = \begin{cases} x_i S(\mathbf{x}) + \frac{x_i - c_i}{a_i^2} (x_i^2 + 1), & k = i, \\ \frac{x_k - c_k}{a_k^2} (x_i^2 + 1), & k \neq i. \end{cases}$$

When $S(\mathbf{x}) = 0$, $\text{rank}(J(\mathbf{x})) = 1$, so we expect the Jacobian to be rank-deficient in a neighborhood of the solution.

If $\mathbf{a} = \mathbf{e} = (1, \dots, 1)^T$, the locus of the solutions is the n -sphere centered in \mathbf{c} with unitary radius. If $\mathbf{c} = 2\mathbf{e}$, the minimal-norm solution is

$$\mathbf{x}^\dagger = \left(2 - \frac{\sqrt{n}}{n} \right) \mathbf{e},$$

while if $\mathbf{c} = (2, 0, \dots, 0)^T$ it is $\mathbf{x}^\dagger = (1, 0, \dots, 0)^T$.

Table 6.3 displays the results for the last case, when $m = 8$ and $n = 10$. These results aim at underlining the importance of estimating the rank of the Jacobian J_k . The implementations of the MNGN2 algorithm are more or less equivalent, recovering solutions with almost optimal norm; MNGN2 $_{\alpha}$ fails in 25% of the tests. The value of η for MNGN2 $_{\alpha\beta}$ is tailored to maximize the performance, which is not possible in practice, while it is automatically estimated for MNGN2 $_{\alpha\beta\delta}$. The MNGN and CKB methods do not perform well, because of the rank deficiency of the Jacobian. We

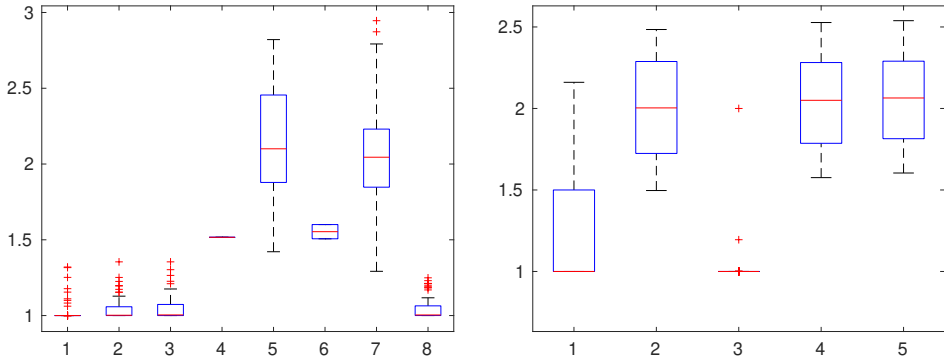


FIGURE 6.1. Boxplot of the norms of the solutions for Examples 6.3 (left) and 6.4 (right). The series are displayed in the same order of Table 6.3 and Table 6.4, respectively.

also implemented the rank estimation in the algorithms from [3]; the corresponding methods are denoted by rCKB. It happens that rCKB₂ produces results comparable to the MNGN2 methods, confirming that a correct estimation of the rank is essential for the convergence, while rCKB₁ converges only in 33% of the tests and produces solutions with large norms. Again, this shows that the sequence adopted for the step length in (r)CKB methods is critical for the effectiveness of the computation.

TABLE 6.3

Results for Example 6.3 with $m = 8$, $n = 10$, $\mathbf{a} = \mathbf{e}$, and $\mathbf{c} = (2, 0, \dots, 0)^T$. In MNGN, CKB₁, and CKB₂, the rank is not estimated.

method	iterations	$\ \tilde{\mathbf{x}}\ $	#success
MNGN2 _{α}	199	1.0210	75
MNGN2 _{$\alpha\beta$} ($\eta = 8$)	206	1.0386	96
MNGN2 _{$\alpha\beta\delta$}	187	1.0460	95
MNGN	173	1.5165	1
CKB ₁	215	2.1506	28
CKB ₂	28	1.5536	2
rCKB ₁	219	2.0770	33
rCKB ₂	195	1.0417	91

The norms of the solutions whose average is displayed in Table 6.3 are reported in the boxplot in the left pane of Figure 6.1. The series are reported in the same order of Table 6.3. In each box, the red mark is the median, the edges of the blue box are the 25th and 75th percentiles, and the black whiskers extend to the most extreme data points non considered to be outliers, which are plotted as red crosses.

EXAMPLE 6.4.

Let F be a nonlinear function such as (6.1), with

$$F_i(\mathbf{x}) = S(\mathbf{x})(x_i - c_i), \quad i = 1, \dots, m, \quad (6.2)$$

and $S(\mathbf{x})$ defined as in the previous example. The first order derivatives of $F_i(\mathbf{x})$ are

$$\frac{\partial F_i}{\partial x_k} = \begin{cases} \frac{2}{a_i^2}(x_i - c_i)^2 + S(\mathbf{x}), & k = i, \\ \frac{2}{a_k^2}(x_k - c_k)(x_i - c_i), & k \neq i. \end{cases}$$

Setting $y_i = x_i - c_i$, for $i = 1, \dots, m$, and $z_j = \frac{x_j - c_j}{a_j^2}$, for $j = 1, \dots, n$, the Jacobian matrix can be represented as

$$J(\mathbf{x}) = S(\mathbf{x})I_{m \times n} + 2\mathbf{y}\mathbf{z}^T,$$

where $I_{m \times n}$ includes the first m rows of an identity matrix of size n . The Jacobian turns out to be a diagonal plus rank-1 matrix. This structure may be useful to reduce complexity when solving large scale problems.

When $S(\mathbf{x}) = 0$, the matrix $J(\mathbf{x})$ has rank 1. Indeed, in this case the compact SVD of the Jacobian is

$$J(\mathbf{x}) = \frac{\mathbf{y}}{\|\mathbf{y}\|} (2\|\mathbf{y}\|\|\mathbf{z}\|) \frac{\mathbf{z}^T}{\|\mathbf{z}\|},$$

so that the only non-zero singular value is $2\|\mathbf{y}\|\|\mathbf{z}\|$. As in the preceding example, we may assume that the Jacobian is rank-deficient in the surroundings of a solution.

The locus of the solutions is the union of the n -ellipsoid and the intersection between the planes $x_i = c_i$, $i = 1, \dots, m$.

If $\mathbf{a} = \mathbf{e}$ and $\mathbf{c} = 2\mathbf{e}$, the minimal-norm solution \mathbf{x}^\dagger depends on the dimensions m and n : if $m < n - \sqrt{n} + \frac{1}{4}$, then it is

$$\mathbf{x}^\dagger = (\underbrace{2, 2, \dots, 2}_m, \underbrace{0, \dots, 0}_{n-m})^T,$$

otherwise, it is

$$\mathbf{x}^\dagger = \left(2 - \frac{\sqrt{n}}{n}\right) \mathbf{e}. \quad (6.3)$$

If $\mathbf{c} = (2, 0, \dots, 0)^T$, it is $\mathbf{x}^\dagger = (1, 0, \dots, 0)^T$. The case $m = 2$, $n = 3$, is displayed in Figure 6.2, together with the iterations of the algorithms MNGN2 $_{\alpha\beta\delta}$ and rCKB₁. In this test, the latter algorithm converges to a solution of non-minimal norm.

Table 6.4 illustrates the situation where $\mathbf{a} = \mathbf{e}$, $\mathbf{c} = (2, 0, \dots, 0)^T$, $m = 8$ and $n = 10$. The corresponding boxplot of the norms of the solutions is displayed in the right pane of Figure 6.1. The MNGN2 $_{\alpha\beta\delta}$ method is the only one which recovers the correct solution; MNGN2 $_\alpha$ gets close to it, but with a very small number of successes.

Table 6.5 reports the results obtained for $\mathbf{a} = \mathbf{e}$ and $\mathbf{c} = 2\mathbf{e}$. In this case, the solution is (6.3). We applied the algorithms to both the solution of the minimal-norm problem, and the computation of the minimal- L -norm solution with $L = D_2$, i.e., the discrete approximations of the second derivative (1.5). Since the solution is exactly in the null space of L , we expect the minimal- L -norm solution to perform well. No algorithm is accurate when $L = I$, as the minimal norm is $2\sqrt{n} - 1 = 5.3246$. When $L = D_2$, the two MNGN2 implementation are superior to the rCKB methods, as $\|L\mathbf{x}^\dagger\| = 0$. As in the previous example, MNGN2 $_\alpha$ exhibits a large number of failures.

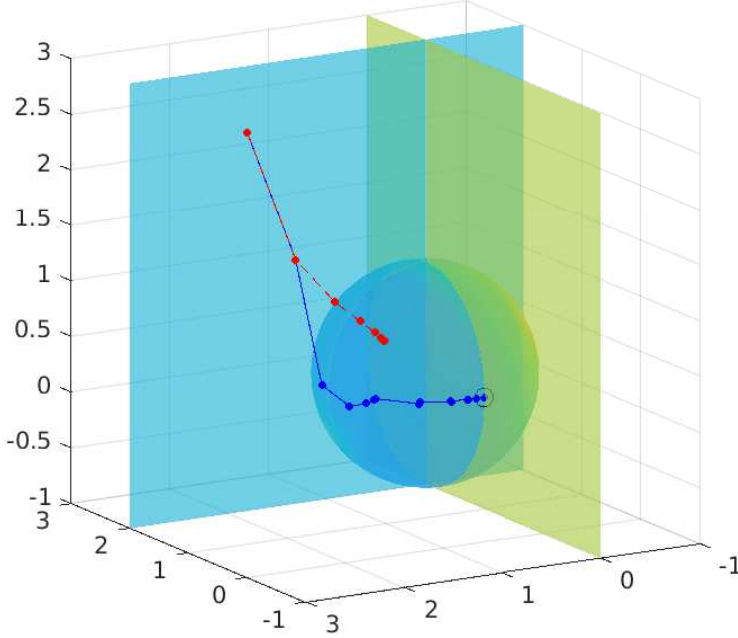


FIGURE 6.2. Solution of problem (6.2) (Example 6.4) for $m = 2$ and $n = 3$, with $\mathbf{a} = (1, 1, 1)^T$, $\mathbf{c} = (2, 0, 0)^T$, and $\mathbf{x}^{(0)} = (0, 3, 3)^T$. The locus of the solutions is the sphere and the line intersection of the two planes. The blue dots are the iterations of the $\text{MNGN2}_{\alpha\beta\delta}$ method, and the red ones correspond to the rCKB_1 method. The black circle encompasses the minimal-norm solution.

TABLE 6.4
Results for Example 6.4 with $m = 8$, $n = 10$, $\mathbf{a} = \mathbf{e}$, and $\mathbf{c} = (2, 0, \dots, 0)^T$.

method	iterations	$\ \tilde{\mathbf{x}}\ $	#success
MNGN2_α	260	1.2701	8
$\text{MNGN2}_{\alpha\beta} (\eta = 8)$	12	2.0014	100
$\text{MNGN2}_{\alpha\beta\delta}$	51	1.0119	100
rCKB_1	27	2.0366	100
rCKB_2	11	2.0531	100

Since this example is interesting in itself as a test problem, we report some further comments on it. If $m = n$, the locus of the solutions is the union of the n -ellipsoid and the point $\mathbf{x} = \mathbf{c}$. The spectrum of $J(\mathbf{x})$ is

$$\sigma(J(\mathbf{x})) = \{S(\mathbf{x}) + 2\mathbf{y}^T \mathbf{z}, S(\mathbf{x}), \dots, S(\mathbf{x})\},$$

where the eigenvalue $S(\mathbf{x})$ has algebraic multiplicity $n - 1$. The Jacobian matrix is invertible if and only if $S(\mathbf{x}) \neq 0$. If this condition is met, the inverse is obtained by the Sherman–Morrison formula

$$J(\mathbf{x})^{-1} = \frac{1}{S(\mathbf{x})} I_n - \frac{2}{S(\mathbf{x})(S(\mathbf{x}) + 2\mathbf{z}^T \mathbf{y})} \mathbf{y} \mathbf{z}^T.$$

TABLE 6.5
Results for Example 6.4 with $m = 8$, $n = 10$, $\mathbf{a} = \mathbf{e}$, and $\mathbf{c} = 2\mathbf{e}$.

	method	iterations	$\ L\tilde{\mathbf{x}}\ $	#success
$L = I$	MNGN2 $_{\alpha}$	12	5.6569	23
	MNGN2 $_{\alpha\beta\delta}$	45	5.4529	100
	rCKB $_1$	26	5.7274	100
	rCKB $_2$	11	5.7520	100
$L = D_2$	MNGN2 $_{\alpha}$	20	0.0500	26
	MNGN2 $_{\alpha\beta\delta}$	17	0.0765	100
	rCKB $_1$	27	2.1694	100
	rCKB $_2$	17	2.2761	100

EXAMPLE 6.5.

Let F be the nonlinear function (6.1) with components

$$F_i(\mathbf{x}) = \begin{cases} S(\mathbf{x}), & i = 1, \\ x_{i-1}(x_i - c_i), & i = 2, \dots, m, \end{cases} \quad (6.4)$$

and $S(\mathbf{x})$ defined as above. The first order partial derivatives of $F_i(\mathbf{x})$ are

$$\frac{\partial F_i}{\partial x_k} = \begin{cases} \frac{2}{a_k^2}(x_k - c_k), & i = 1, k = 1, \dots, n, \\ x_i - c_i, & i = 2, \dots, m, k = i - 1, \\ x_{i-1}, & i = k = 2, \dots, m, \\ 0, & \text{otherwise.} \end{cases}$$

Setting $z_j = 2\frac{x_j - c_j}{a_j^2}$ and $y_j = x_j - c_j$, for $j = 1, \dots, n$, the Jacobian matrix of F is

$$J(\mathbf{x}) = \begin{bmatrix} z_1 & z_2 & z_3 & \cdots & z_{m-1} & z_m & \cdots & z_n \\ y_2 & x_1 & & & & & & \\ y_3 & x_2 & & & & & & \\ & \ddots & \ddots & & & & & \\ & & & \ddots & \ddots & & & \\ & & & & & y_m & x_{m-1} & \end{bmatrix}. \quad (6.5)$$

The locus of the solutions is the intersection between the hypersurface defined by $S(\mathbf{x}) = 0$ and by the pairs of planes $x_{i-1} = 0$, $x_i - c_i = 0$, $i = 2, \dots, m$.

If $\mathbf{a} = \mathbf{e} = (1, \dots, 1)^T$ and $\mathbf{c} = 2\mathbf{e}$, the minimal-norm solution is

$$\mathbf{x}^\dagger = \left(\xi_{n,m}, \underbrace{2, \dots, 2}_{m-1}, \underbrace{\xi_{n,m}, \dots, \xi_{n,m}}_{n-m} \right)^T, \quad (6.6)$$

with $\xi_{n,m} = 2 - (n - m + 1)^{-1/2}$, while if $\mathbf{c} = (2, 0, \dots, 0)^T$ it is $\mathbf{x}^\dagger = (1, 0, \dots, 0)^T$. It is immediate to observe that in the last situation the Jacobian (6.5) is rank-deficient at \mathbf{x}^\dagger . This case is illustrated in Figure 6.3, where the iterations of the MNGN2 $_{\alpha\beta\delta}$ and the rCKB $_1$ methods are reported too. The iterations performed are 20 and 24, respectively; the computed solutions are substantially coincident.

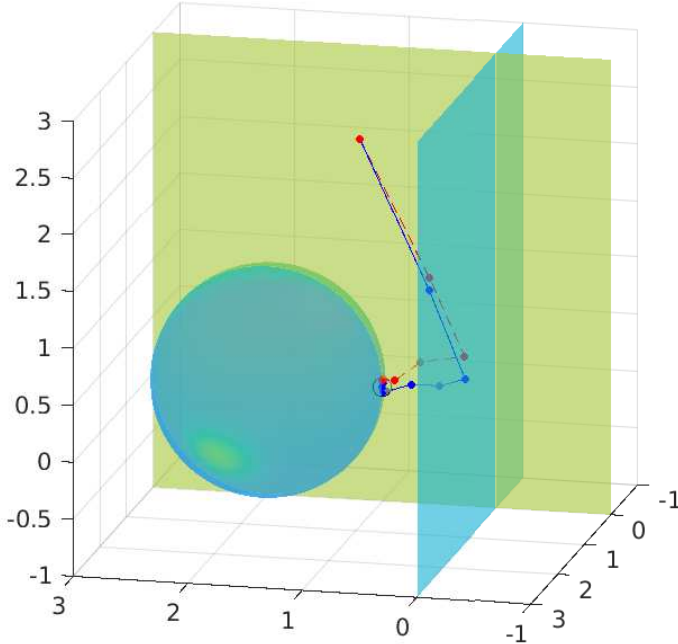


FIGURE 6.3. *Solution of problem (6.4) (Example 6.5) for $m = 2$ and $n = 3$, with $\mathbf{a} = (1, 1, 1)^T$, $\mathbf{c} = (2, 0, 0)^T$, and $\mathbf{x}^{(0)} = (\frac{1}{2}, 3, 3)^T$. The solutions are in the intersection between the sphere and the union of the two planes. The blue dots are the iterations of the $\text{MNGN2}_{\alpha\beta\delta}$ method, and the red ones correspond to the rCKB_1 method. The black circle encompasses the minimal-norm solution.*

Table 6.6 displays the results obtained for the same parameter vectors of Figure 6.3, when the size of the problem varies, i.e., for $(m, n) = (8k, 10k)$, $k = 1, 2, 3$. The MNGN2 algorithms behave almost optimally, while the rCKB methods lead to solutions with larger norm. The table shows that the performance is not significantly affected by the size of the problem. This example suggests that large scale problems could be faced by the methods discussed, but a suitable algorithm for the solution of the linearized problem should be adopted, to reduce the computational complexity of each step. This aspect will be the object of future research.

Table 6.7 investigates the effectiveness of choosing an appropriate model profile $\bar{\mathbf{x}}$ when applying the MNGN2 algorithms. We consider the case $\mathbf{a} = \mathbf{e}$, $\mathbf{c} = 2\mathbf{e}$, $m = 8$, and $n = 10$. The minimal-norm solution \mathbf{x}^\dagger is (6.6), with $\xi_{8,10} \simeq 1.4226$ and $\|\mathbf{x}^\dagger\| \simeq 5.8371$.

When $\bar{\mathbf{x}} = \mathbf{0}$, the solutions produced by the considered variants of the method are almost optimal, but the number of iterations is quite large, as well as the number of failures for $\text{MNGN2}_{\alpha\beta}$ (with a suitably chosen η) and $\text{MNGN2}_{\alpha\beta\delta}$. The model profile $\bar{\mathbf{x}} = 2\mathbf{e}$ reduces the number of iterations and leads to almost 100% of successes, but the average norm of the solutions is slightly larger than the optimal one. Choosing $\bar{\mathbf{x}} = 1.7\mathbf{e}$, a value which is roughly halfway between 2 and $\xi_{8,10}$, the extreme values of \mathbf{x}^\dagger , restores the optimality of the results. This confirms that, when a priori information is available, an accurate choice of the model profile enhances the performance of the

TABLE 6.6
Results for Example 6.5 with different size (m, n) , $\mathbf{a} = \mathbf{e}$, and $\mathbf{c} = (2, 0, \dots, 0)^T$.

(m, n)	method	iterations	$\ \tilde{\mathbf{x}}\ $	#success
(8, 10)	MNGN2 $_{\alpha}$	167	1.0000	48
	MNGN2 $_{\alpha\beta}$ ($\eta = 8$)	24	1.0508	100
	MNGN2 $_{\alpha\beta\delta}$	37	1.0659	100
	rCKB $_1$	44	1.4867	100
	rCKB $_2$	22	1.4776	100
(16, 20)	MNGN2 $_{\alpha}$	144	1.0000	36
	MNGN2 $_{\alpha\beta}$ ($\eta = 8$)	29	1.0170	99
	MNGN2 $_{\alpha\beta\delta}$	34	1.0518	99
	rCKB $_1$	54	1.4343	100
	rCKB $_2$	53	1.5269	90
(24, 30)	MNGN2 $_{\alpha}$	133	1.0000	34
	MNGN2 $_{\alpha\beta}$ ($\eta = 8$)	34	1.0154	99
	MNGN2 $_{\alpha\beta\delta}$	32	1.0191	96
	rCKB $_1$	43	1.4446	100
	rCKB $_2$	52	1.4529	70

algorithms.

TABLE 6.7
Results for Example 6.5 with $m = 8$, $n = 10$, $\mathbf{a} = \mathbf{e}$, and $\mathbf{c} = 2\mathbf{e}$.

	method	iterations	$\ \tilde{\mathbf{x}}\ $	#success
$\bar{\mathbf{x}} = \mathbf{0}$	MNGN2 $_{\alpha}$	138	5.8371	100
	MNGN2 $_{\alpha\beta}$ ($\eta = 8$)	175	5.8374	38
	MNGN2 $_{\alpha\beta\delta}$	94	5.8988	67
$\bar{\mathbf{x}} = 2\mathbf{e}$	MNGN2 $_{\alpha}$	37	6.1141	99
	MNGN2 $_{\alpha\beta}$ ($\eta = 8$)	34	6.1144	98
	MNGN2 $_{\alpha\beta\delta}$	34	6.1144	98
$\bar{\mathbf{x}} = 1.7\mathbf{e}$	MNGN2 $_{\alpha}$	54	5.8371	100
	MNGN2 $_{\alpha\beta}$ ($\eta = 8$)	34	5.8394	99
	MNGN2 $_{\alpha\beta\delta}$	40	5.8789	99

7. Conclusions. This paper explores the computation of the minimal- (L) -norm solution of nonlinear least-squares problems, and the reasons for the occasional lack of convergence of Gauss–Newton methods. We propose an automatic procedure to estimate the rank of the Jacobian along the iteration, and the introduction of two different relaxation parameters that improve the efficiency of the iterative method. The first parameter is determined by applying the Armijo–Goldstein principle, while three techniques are investigated to estimate the second one. In numerical experiments performed on various test problems, the new methods prove to be very effective, compared to other approaches based on a single damping parameter. In particular, the variant which automatically estimates the projection parameter gives satisfactory results in all the examples.

Acknowledgements. The authors are indebted to two anonymous reviewers, whose remarks were essential for improving both the content and the presentation

of this paper. We thank Maurizio Ruggiu for suggesting the problem reported in Example 6.1. The work of the authors was partially supported by the Regione Autonoma della Sardegna research project “Algorithms and Models for Imaging Science [AMIS]” (RASSR57257, intervento finanziato con risorse FSC 2014-2020 - Patto per lo Sviluppo della Regione Sardegna), and the INdAM-GNCS research project “Tecniche numeriche per l’analisi delle reti complesse e lo studio dei problemi inversi”. Federica Pes gratefully acknowledges CRS4 (Centro di Ricerca, Sviluppo e Studi Superiori in Sardegna) for the financial support of her Ph.D. scholarship.

REFERENCES

- [1] L. ARMJO, *Minimization of functions having Lipschitz continuous first partial derivatives*, Pac. J. Math., 16 (1966), pp. 1–3.
- [2] Å. BJÖRK, *Numerical Methods for Least Squares Problems*, SIAM, Philadelphia, 1996.
- [3] S. L. CAMPBELL, P. KUNKEL, AND K. BOBINYEC, *A minimal norm corrected underdetermined Gauß–Newton procedure*, Applied Numerical Mathematics, 62 (2012), pp. 592–605.
- [4] A. CONCAS, S. NOSCHESE, L. REICHEL, AND G. RODRIGUEZ, *A spectral method for bipartizing a network and detecting a large anti-community*, J. Comput. Appl. Math., 373 (2020), p. 112306 (15 pages).
- [5] J. E. DENNIS JR. AND R. B. SCHNABEL, *Numerical methods for unconstrained optimization and nonlinear equations*, SIAM, 1996.
- [6] J. ERIKSSON, *Optimization and Regularization of Nonlinear Least Squares Problems*. Ph.D. Thesis, Umeå University, Sweden, 1996.
- [7] J. ERIKSSON AND P. A. WEDIN, *Regularization methods for nonlinear least squares problems. part i: Exactly rank-deficient problems*, tech. rep., Umeå University, Sweden, 1996.
- [8] J. ERIKSSON, P. A. WEDIN, M. E. GULLIKSSON, AND I. SÖDERKVIST, *Regularization methods for uniformly rank-deficient nonlinear least-squares problems*, J. Optim. Theory Appl., 127 (2005), pp. 1–26.
- [9] A. A. GOLDSTEIN, *Constructive Real Analysis*, Harper and Row, 1967.
- [10] G. H. GOLUB AND C. F. VAN LOAN, *Matrix Computations*, The John Hopkins University Press, Baltimore, third ed., 1996.
- [11] P. C. HANSEN, *Rank–Deficient and Discrete Ill–Posed Problems*, SIAM, Philadelphia, 1998.
- [12] P. C. HANSEN, V. PEREYRA, AND G. SCHERER, *Least Squares Data Fitting with Applications*, Johns Hopkins University Press, Baltimore, 2012.
- [13] J. M. ORTEGA AND W. C. RHEINBOLDT, *Iterative Solution of Nonlinear Equations in Several Variables*, Academic Press, New York, 1970.
- [14] F. PES AND G. RODRIGUEZ, *The minimal-norm Gauss-Newton method and some of its regularized variants*, Electron. Trans. Numer. Anal., 53 (2020), pp. 459–480.
- [15] L. REICHEL AND G. RODRIGUEZ, *Old and new parameter choice rules for discrete ill-posed problems*, Numer. Algorithms, 63 (2013), pp. 65–87.